

Relativistic quantum dynamics in strong fields: Photon emission from heavy, few-electron ions

S Fritzsche¹, P Indelicato² and Th Stöhlker³

¹ Institut für Physik, Universität Kassel, Heinrich-Plett-Str. 40, D-34132 Kassel, Germany

² Laboratoire Kastler Brossel, École Normale Supérieure et Université Pierre et Marie Curie, Boite 74, 4 Place Jussieu, F-75252 Paris CEDEX 05, France

³ Gesellschaft für Schwerionenforschung (GSI), D-64291 Darmstadt, Germany, Institut für Kernphysik University of Frankfurt, 60486 Frankfurt, Germany

Abstract. Recent progress in the study of the photon emission from highly-charged heavy ions is reviewed. These investigations show that high- Z ions provide a unique tool for improving the understanding of the electron-electron and electron-photon interaction in the presence of strong fields. Apart from the bound-state transitions, which are accurately described in the framework of Quantum Electrodynamics, much information has been obtained also from the radiative capture of (quasi-) free electrons by high- Z ions. Many features in the observed spectra hereby confirm the inherently *relativistic* behavior of even the simplest compound quantum systems in Nature.

PACS numbers: 32.10.-f, 34.70.+e, 34.80.Lx

1. Introduction

Hundred years after Einstein put forth his ideas about relativity and the particle nature of light, the photon emission from highly-charged, heavy ions has been found a unique and very exciting framework for studying his visionary concepts in detail. The gradual discovery that only the combination of relativity with the photon picture in the framework of quantum mechanics (the theory that was needed to understand the microscopic world) could describe the interaction between light and matter in all its diversity is well exemplified by recent case studies on high- Z ions. This combination has lead also to Quantum Electrodynamics (QED), the most accurate and successful theory in physics today, and served as model for those Field Theories that now compose the Standard Model. *Relativistic* transformations are also required to interpret the experiments with high-energetic ions, if their speed becomes a sizeable fraction of the speed of light. Indeed, experiments using Laser spectroscopy at ions storage rings have enabled to test with high accuracy time dilation (Saathoff et al. 2003). Born less than 3 decades ago, the field of highly charged ions is therefore a tribute to Einstein's work.

Today, there are two research lines for which the observed photon spectra are crucial for our present understanding of the light-matter interaction in the presence of strong fields. They are related to the electronic *structure* and *dynamics* of high- Z ions and to great improvements in the accuracy of the experiments. Our (theoretical) understanding of atoms and ions has advanced considerably during the last decade thanks, for example, to the study of x-ray transitions between bound states of high- Z ions. These investigations have established heavy few-electron ions as a privileged tool owing to the strong enhancement of QED and other relativistic effects by large powers in $(Z\alpha)$.

In relativistic ion-atom collisions, in addition, much details about the electron-photon interaction in strong fields were obtained from the radiative capture of free (or quasi-free) electrons (REC). At storage rings, this electron capture determines not only the lifetimes but also provides information about the magnetic components of the radiation field and the coupling of the spin and orbital motion of the electrons. Recent experimental and theoretical advances showed, furthermore, that REC may provide a tool for controlling the polarization of ions beams.

In this contribution, the recent progress in the study of the photon emission from highly-charged heavy ions is reviewed. After a short summary on the experimental facilities for heavy-ion research in Sec. 2, the photon emission from bound-bound transitions is discussed in Sec. 3, including the Quantum Electrodynamic corrections to the transition energies as well as the one- and two-photon emission from high- Z ions. In Sec. 4, we review the radiative capture of free electrons with some emphasis on the polarization of the emitted radiation and the alignment of the residual ions, if the capture occurs into an excited state of the ion. Conclusions and outlook onto future experiments are finally given in Sec. 5.

2. Experimental heavy ion facilities

The current progress in the basic fields of atomic collision- and structure-research involving highly charged heavy ions is closely related to the application of modern ion source and accelerator techniques as well as to the use of advanced detection techniques for photons, electrons and recoil ions. During the last few years the development of storage rings equipped with electron-cooler devices (Franzke 1987, Franzke 1990, Bosch 1993, Mokler & Stöhlker 1996, Steck et al. 2004) and electron beam driven ion traps have received a lot of attention (Schneider et al. 1989, Marrs, Beiersdorfer & Schneider 1994, Marrs, Elliott & Knapp 1994, Gillaspy 2001). For the heaviest ions such as hydrogenlike uranium, a quantum leap was achieved with the advent of the heavy-ion storage ring ESR at GSI in Darmstadt (see Fig. 1) and the Super-EBIT at Livermore. At the ESR, electron cooling guarantees for ion beams of unprecedented quality, i.e. this technique provides cooled and intense beams at high- Z and with precisely known energies and charge states at small momentum spread (Bosch 1993, Mokler & Stöhlker 1996, Steck et al. 2004). These conditions are in particular well suited for the spectroscopy of x-ray transitions in the heaviest H-like ions. In contrast to storage rings, at EBIT devices, the highly charged ions are produced at rest in the laboratory. There, the experiments focus on QED and atomic structure studies for heavy few-electron ions (Beiersdorfer et al. 1993, Beiersdorfer et al. 1995, Gillaspy 2001).

In the following, we concentrate on the experimental techniques at the heavy-ion storage ring ESR where radiative recombination and REC transitions have become a subject of detailed experimental investigations. At the ESR, interaction of the ion beams with matter can be studied under single collision conditions at the internal gasjet target where particle densities of about 10^{12}p/cm^3 are provided. This can be compared with a typical density of a solid state target of about 10^{21}p/cm^3 . Most important and in contrast to conventional single-pass experiments where direct beams from relativistic accelerators are used, no active or passive beam collimation is required at the ESR. Thus, experimental conditions are almost completely background-free. A further unique feature of the ESR is the deceleration capability of the storage ring. It enables to perform atomic collision experiments for highly-charged ions in a completely new energy and charge-state domain, i.e. for highest atomic charges (e.g. U^{92+}) at energies far below their production energy (Stöhlker et al. 1998, Steck et al. 2004). In this low-energy domain, the perturbation Q/v (Q and v the charge and the velocity, respectively) caused by the projectile reaches values otherwise not accessible at accelerators. Furthermore, the deceleration technique turned out to be indispensable for accurate precision spectroscopy aiming for a test of QED at high- Z H-like ions such as H-like uranium. For low-energetic ion beams the relativistic Doppler corrections are strongly reduced whereas at high energies the Doppler effect is a serious limitation for such studies. As an example, by applying this technique for U^{92+} a beam energy of 3 MeV/u could already be achieved (corresponding to a velocity of 8% of the speed of light c) (Steck et al. 2004) which has to be compared with the production energy for

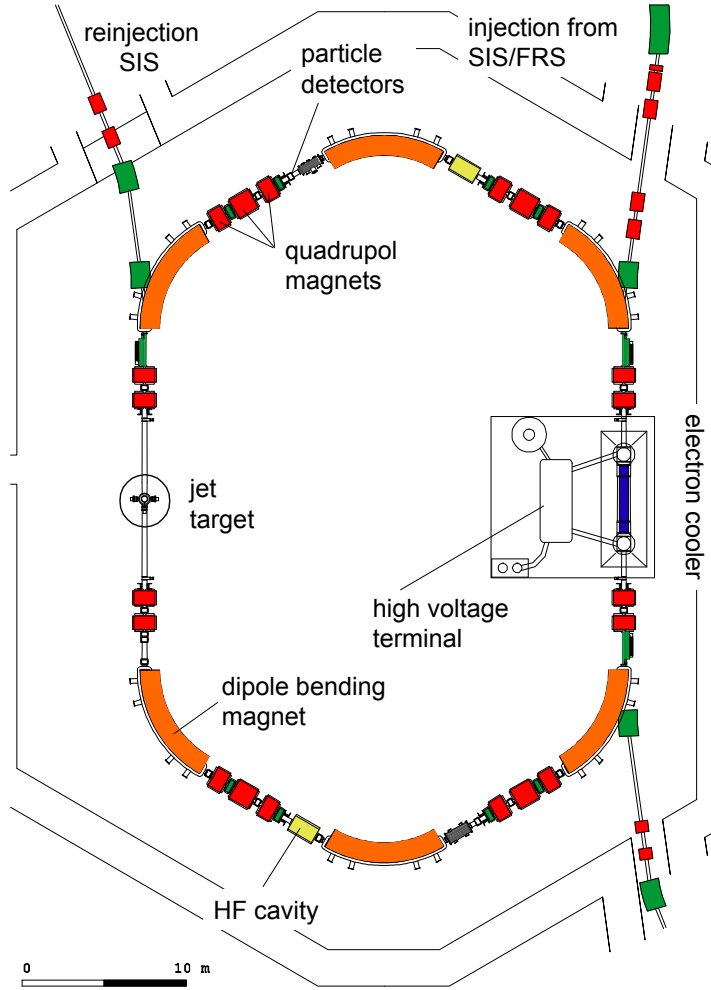


Figure 1. Schematic presentation of the storage and cooler ring ESR at GSI-Darmstadt. The layout depicts the beam guiding system (dipole bending magnets, quadrupoles and hexapoles) as well as the most important installations for beam handling and diagnostics (kicker, rf cavities, Schottky noise pick up, electron cooler). The position of the internal jet-target is marked in addition.

the bare charge state of 400 MeV/u (71% of c).

During the last decade, the progress in storage ring and cooling techniques was accompanied by an impressive development of position and energy sensitive solid state detectors for advanced photon spectroscopy. The tremendous progress in this field of detector design, which took place very recently, is mainly motivated by the demands for efficient γ - and x-ray spectrometers, in connection with the need for such devices that arises in applied research such as medical imaging. The properties of such detectors are millimeter to sub-millimeter spatial resolution as well as time and energy resolution in the hard x-ray energy regime above 15 keV (Protic et al. 2001, Stöhlker et al. 2003). Combined with a focusing crystal spectrometer, for example, these detectors make possible the measurement of an energy spectrum wide enough to investigate

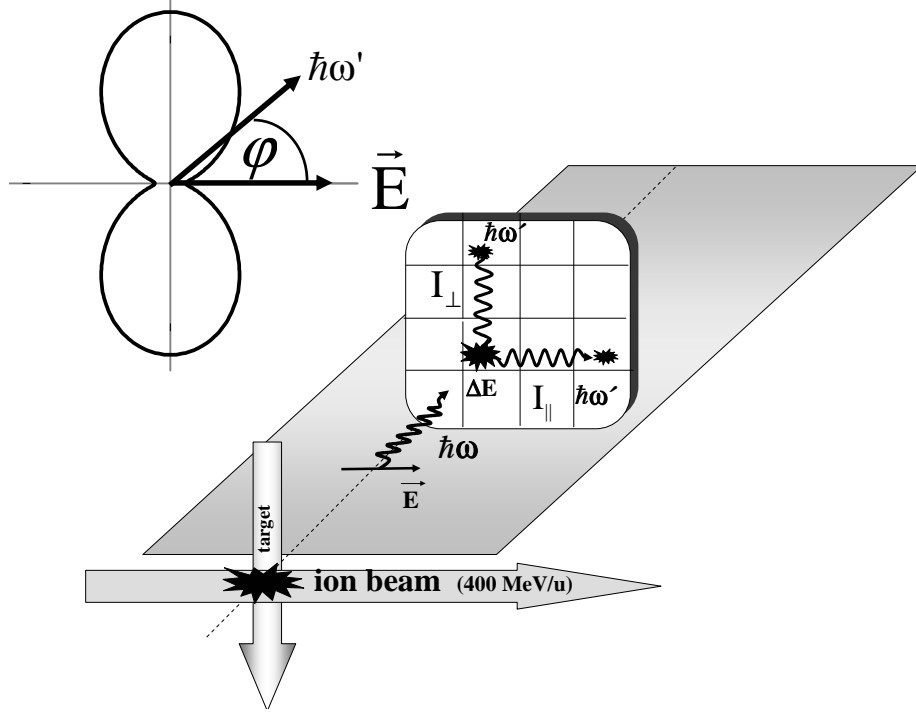


Figure 2. Detector geometry used for the measurement of the linear photon polarization for K-REC at 400 MeV/u $U^{92+} \rightarrow N_2$ collisions by exploiting the Compton effect (see also Sec. 4.2) (Stöhlker et al. 2004, Tachenov et al. 2004).

the whole energy range of interest simultaneously (Beyer et al. 2004). Very recently, moreover, a microstrip detector system was developed at the Forschungszentrum Jülich (Protic et al. 2001) with a position resolution of close to 200 μm which has become available for the high-precision x-ray spectroscopy at the ESR storage ring (Stöhlker et al. 2003, Beyer et al. 2004). Along with a new kind of transmission crystal spectrometer (Beyer et al. 2004), such detectors may play a key role for a precise test of quantum electrodynamics in the heaviest one-electron systems. Another very important feature of granular, position sensitive systems is their sensitivity to the photon polarization at energies above 100 keV. Using two-dimensional solid-state detectors, it was shown recently that the polarization of bound-bound and free-bound transitions in highly-charged heavy ions can be measured with high accuracy by exploiting the Compton scattering within the detector (Stöhlker et al. 2004). This is illustrated in Fig. 2, where the detection geometry for a polarization experiment is displayed, using a germanium pixel detector (see also Sec. 4.2).

3. Relativistic and Quantum Electrodynamics effects in photon emission

The photon emission from highly charged ions has many specific aspects which all related to the fact that the speed of the electron on its orbit is of order $Z\alpha c$, which is worth 66 % of the speed of light for the 1s shell of uranium. The relativistic effects enter

the transition rates by both the transition energy and the operator. In this section we summarize a number of theoretical considerations for both energies and transition rates and discuss a number of experimental results.

3.1. Quantum Electrodynamics corrections to transition energies

Relativistic Quantum theory really started when Dirac (1928) proposed the equation bearing his name. Because he started from the relation between mass, impulsion and energy, $E^2 = m^2c^4 + p^2c^2$, introduced by Einstein's relativity, Dirac found that his equation had both positive and negative energy solutions. He was thus lead to the concept of the Dirac *electron sea* to avoid transitions from positive energy states to negative energy ones. Soon, moreover, the relativistic form of the electron-electron interaction was investigated by Breit (1929). The existence of the Dirac sea lead to the idea of Vacuum Polarization, that had calculable effect on atomic level energies (Uehling 1935). Yet the theory was plagued by infinities showing up in all sorts of perturbation expansions. The experiment of Lamb & Retherford (1950) showing that the Dirac equation could not predict correctly the fine structure of hydrogen was one of the experiments that lead to QED. After the first evaluation of the self-energy by Bethe (1947), the Lamb shift was calculated more and more accurately in the framework of non-relativistic QED (NRQED) for many years, as a series in $Z\alpha$. It is only in the 70's that Mohr (1974) showed, by performing the first high-precision, all-order calculation of the $1s$ Lamb-shift, that the NRQED $Z\alpha$ expansion did not converge, even for moderately large $Z \geq 10$. Since then a considerable amount of non-perturbative QED calculations have been performed for heavy one- and few-electron ions, including a complete calculations of QED corrections of order α^2 , e.g., two loop self-energy, see Yerokhin et al. (2003b) and references therein. For a review of non-perturbative, one-electron QED calculations, see, e.g., Mohr et al. (1998). A few years later, a series of experiments measuring the hydrogen-like ions $1s$ Lamb shift started, the first one being performed at the BEVALAC in Berkeley (Briand et al. 1990). Within the past 14 years, thanks to the use of heavy-ion storage rings, the experimental accuracy for the $1s$ Lamb-shift has improved by a factor of 25, although it cannot yet match theoretical accuracy (Fig. 3). The most recent values for the different QED and nuclear corrections to the $1s$ Lamb shift in hydrogen-like uranium are presented in Table 1 and compared with recent experimental results obtained at ESR.

Following the first experiment on Lithium-like uranium (Schweppe et al. 1991), a large effort has also been made in the evaluation of QED corrections for three-electron systems (Indelicato & Mohr 1991, Cheng et al. 1991, Cheng et al. 1993, Yerokhin et al. 1998, Yerokhin et al. 1999, Yerokhin et al. 2000, Indelicato & Mohr 2001). Simultaneously the use of electron storage rings provided many accurate measurements (Brandau et al. 2003). In principle, QED is the theory of choice to perform such calculations for heavy ions. Yet, as soon as a high accuracy is required, QED cannot be used alone in practice, even for relatively large Z . This is because the real behavior of

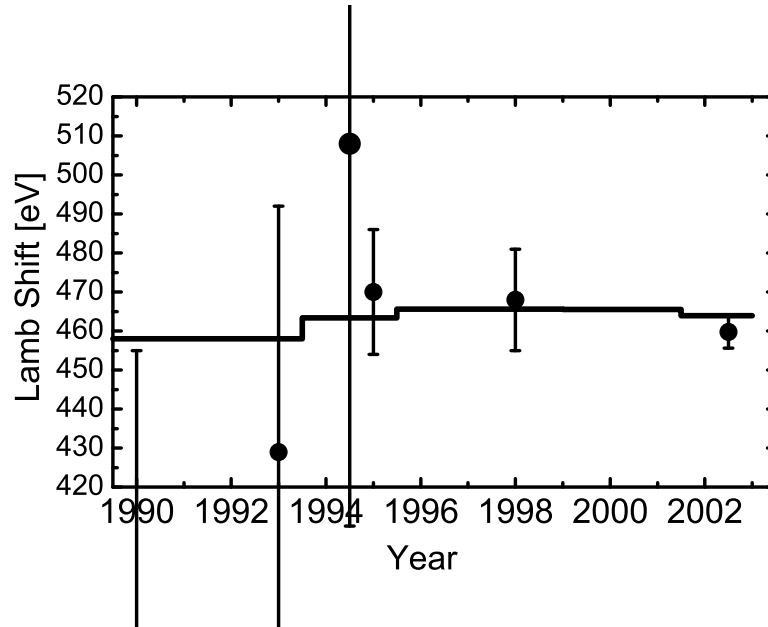


Figure 3. Evolution of the accuracy of the Lamb shift measurements and the calculations (solid line) over time for hydrogen-like uranium [see Gumberidze et al. (2004) and Refs. therein].

the corrections corresponding to n exchanged photons between two interacting electrons is only $1/Z^n$ while a naive look at the corresponding Feynmann diagrams would lead to expect a dependence in α^n . One would then have to evaluate Feynman diagrams of very high order to reach an acceptable precision, which is impossible with presently known QED techniques, although some explorations are being done (Lindgren 2000). In practice, therefore, one has to resort to relativistic many-body methods like Relativistic Many Body Perturbation Theory (RMBPT), Relativistic Configuration Interaction (RCI) and Multi-Configuration Dirac-Fock (MCDF), which are described in Sec. 3.2, and to correct for missing QED contributions order by order if doable.

3.2. Relativistic Many-Body issues

The need for relativistic self-consistent field technique was felt soon after the introduction of the Dirac equation (Swirles 1935). At first the relativistic many-body techniques were developed from their non-relativistic counterparts, replacing the Schrödinger operator by the Dirac one, and replacing the Coulomb interaction between the electrons by the Breit interaction.

Over the years relativistic calculations evolved until the development of the MCDF method by Grant (1970) and Desclaux (1975). Because this method is very general and (easily) provides a large fraction of the many-body contributions, the so-called correlation energy, it became rapidly popular. Yet its ties to QED and the role of the negative energy states, inherent to the use of the Dirac equation, was not considered for some years. The existence of negative energy states lead to a problem known as

Table 1. Contributions to the $1s$ Lamb shift of Hydrogen-like uranium (Yerokhin et al. 2003a). SE: Self-energy; Uehling: Vacuum polarization in the Uehling approximation; WK: Wichmann and Kroll correction to vacuum polarization; Fin. Size: effect of the nuclear charge distribution, assuming a mean spherical radius of 5.860(2) Fm; Nucl. Pol.: nuclear polarization (Plunien & Soff 1995); two-loop: sum of all QED corrections of order α^2 . Experimental value from (Gumberidze et al. 2004).

	Contrib.	Value (eV)
α QED	SE	355.046
	Uehling	−93.597
	WK	4.975(2)
α^2 QED	Two-loop	−1.26(33)
	Recoil	0.46
Nucl. Effects	Fin. Size	198.79(40)
	Nucl. Pol.	−0.19(9)
	total	464.22(53)
	experiment	460.2(4.6)

continuum dissolution (Brown & Ravenhall 1951, Sucher 1980): treatment to all orders using an electron-electron interaction operator that couple positive and negative energy states (which is the case of even the Coulomb interaction) lead to infinities. No rigorous solution to this problem can be found outside of QED. Indeed, derivation of the many-electron Hamiltonian from QED shows that the electron-electron interaction *must* be “sandwiched” between projection operators on the positive energy states. It is only recently that the push toward high- Z few-electron ion experiments prompted a study on how continuum dissolution happens in MCDF calculation and how to implement projection operators (Indelicato 1995).

Relativistic Many-Body Perturbation Theory evolved originally from the non-relativistic work by Kelly (1963) and Lindgren (1974). Early calculations were performed on lithium-like ions (Johnson et al. 1988). A review on RMBPT techniques and results can be found in (Sapirstein 1998). Hereby, the implementation of projection operators in RMBPT was very natural and mandatory as infinities appear already in second order perturbation theory if such operators are not present (Heully et al. 1986, Heully et al. 1986b).

An other method that has been used in few-electron calculations is the Relativistic Configuration Method (RCI). This method is a variant of the MCDF method, which uses finite basis sets like RMBPT. It was found to be very effective to describe few-electron ions (Chen et al. 1993, Cheng et al. 1994, Johnson et al. 1995, Chen et al. 2001). MCDF and RCI calculations have been tested in experiments realized at the Super-EBIT in Livermore, on transition to the $n = 2$ levels of 3 to 10-electron U and Th ions (Beiersdorfer et al. 1993, Beiersdorfer et al. 1995).

Beside the need for projection operators, there is a number of features that

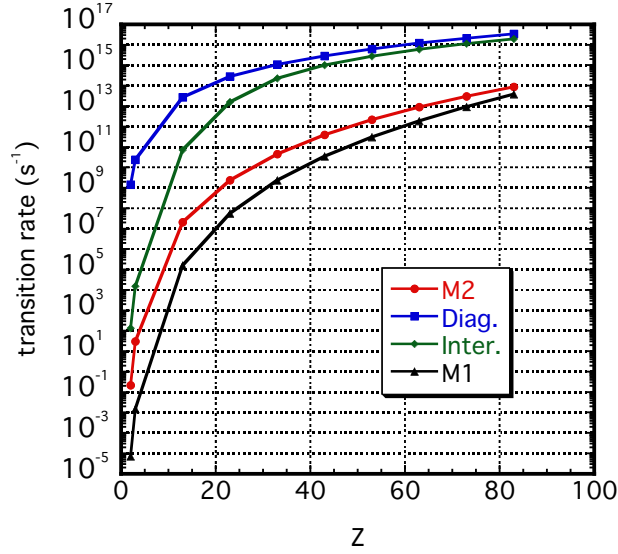


Figure 4. Transition rate for He-like ions (s^{-1}). M₂: $1s2p^3P_2 \rightarrow 1s^2^1S_0$. Diag: diagram line $1s2p^1P_1 \rightarrow 1s^2^1S_0$ (E₁). Inter: intercombination line $1s2p^3P_1 \rightarrow 1s^2^1S_0$ (E₁). M₁: $1s2s^3S_1 \rightarrow 1s^2^1S_0$.

are common to all relativistic many-body calculations. First, the electron-electron interaction contains retardation terms, which is a direct consequence of Einstein’s relativistic theory (finite speed of light). Because each particle in the system must have its own proper time in relativity, there can be no exact Hamiltonian formalism to describe it. This can be seen, for instance, in the expression of the electron-electron interaction operator, which depends on the one-electron orbital energies. These energies are known only when the full solution of the self-consistent field has been found and cannot be defined *a priori* in the many-body formalism.

Because of the multitime nature of the problem, the most general formalism to handle the relativistic many-body problem is the two-time Green’s function formalism of Shabaev (1990). This formalism is needed, in particular, to add QED corrections to the transition rates and other quantities beyond the energies. An alternative formalism has been developed recently (Lindgren et al. 2004), based on covariant evolution operator. At some point, however, QED corrections to second order in the electron-electron interaction must be made (Blundell et al. 1993, Lindgren et al. 1995, Mohr & Sapirstein 2000, Åsén et al. 2002). These corrections partially cancel two-electron self-energy corrections. At present, this interplay between QED and many-body effects constitutes the greatest challenge posed to the accurate theoretical evaluation of transition energies in the field of highly-charged heavy ions.

3.3. One-photon bound-bound radiative transition

Relativistic effects play a central role also in the photon emission. In the helium isoelectronic sequence, for example, the $1s2s^3S_1 \rightarrow 1s^2^1S_0$ line is called the “relativistic M₁” transition because it is completely forbidden in non-relativistic theory. For high-

Z ions, in addition, intercombination lines like $1s2p\ ^3P_1 \rightarrow 1s^2\ ^1S_0$ become almost as intense as the “allowed” transitions, i.e. the diagram line $1s2p\ ^1P_1 \rightarrow 1s^2\ ^1S_0$. The dependence of the transition rates as a function of the atomic number and the successive multipoles, obtained by the expansion of the relativistic transition operator in spherical components, is such that high-multipole transitions can occur with sizeable probabilities. Compared to its non-relativistic equivalents, this operator automatically includes such relativistic effects as retardation. To stay with the example of the helium-like ions, the $1s2p\ ^3P_2 \rightarrow 1s^2\ ^1S_0$ M_2 transition has a relative strength of 1.5×10^{-10} at $Z = 2$, but already 2.5×10^{-3} at $Z = 83$. Some example of the evolution of transition probabilities in helium-like ions are shown on Fig. 4 and more details can be found in Marrus & Mohr (1978). The lifetime of the $1s2s\ ^3S_1$ in He-like Xe has been measured at GANIL to 3 % accuracy (Marrus et al. 1989a) and has been found in good agreement with theory (Johnson et al. 1995a, Indelicato 1996).

In general, the higher-order multipole contributions to a given transition rate can be neglected. However, there are a few cases for which this is not true. For example, in the $3d_{5/2} \rightarrow 2p_{1/2}$ transition in hydrogen-like ions, the M_3 contribution represents between 32 % ($Z = 1$) and 40 % ($Z = 92$) of the dominant E_2 multipole. Similarly, the E_4 multipole contributes between 51 % to 58 % of the $4f_{7/2} \rightarrow 2p_{1/2}$ M_3 transition for these ions. The study of highly-charged heavy ions has enabled one to observe directly forbidden transitions beyond M_2 transitions, which has been observed or relatively low- Z for helium-like ions. For example, magnetic octupole (M_3) transitions have been observed in an EBIT for nickel-like Th and U ions (Beiersdorfer et al. 1991). Even if the contribution of the higher multipoles to the total rate is of the order of 1 %, they can however influence the angular distribution of the emitted photons. Recent experiments on that subject are described in Sec. 4.3.

Transition probabilities in few-electron ions are a very stringent test of relativistic many-body theories. In variational methods like the MCDF method, transition probabilities involve the wavefunction, which is less precisely evaluated than the energy. In the same way as in the evaluation of transition energies, there are several issues that have to be addressed when calculating transitions probabilities. For example, one must also properly account for the negative-energy continuum. This was first noticed for the $1s2s\ ^3S_1 \rightarrow 1s^2\ ^1S_0$ M_1 transition (Indelicato 1996). It was also shown, that in contrast to the non-relativistic case, the full gauge invariance (for example between length and velocity gauge for E_n transitions) can be achieved *only* if the negative energy continuum is properly accounted for (Derevianko et al. 1998). An extra complication, when using highly correlated wavefunctions for evaluating transition probabilities and other operators, is that the orbitals in initial and final wave functions are usually not orthogonal (Cheng & Johnson 1977). This may have a large effect in some transitions like the relativistic M_1 (Indelicato 1996). Other kinds of transitions like two-electron, one-photon transitions, may depend entirely on non-orthogonality between correlated wave functions. A competition between such a transition and an E_2 transition has been predicted and observed in Be-like xenon (Indelicato 1997).

There has been little studies of QED corrections to transition amplitudes. Most of the time, QED corrections are accounted for only by the inclusion of radiative corrections to the energy (which is done automatically when experimental energy are used for the calculation of the transition rates). QED corrections to the $2p \rightarrow 1s$ and $2s \rightarrow 1s$ in hydrogenlike ions have been calculated recently (Sapirstein et al. 2004). These authors have shown that there might be a very strong cancellation between the effect of the energy correction and those of the wavefunction correction. When several electrons are present, there are other kind of QED corrections that needs to be included. For example, the reducible contribution to some transitions in helium-like ions has been investigated (Indelicato et al. 2004) and found to be small.

Forbidden transitions can also be a tool for studying the interaction of the electrons with the nuclear magnetic moments through the hyperfine quenching of the $1s2p\ ^3P_0$ level in heliumlike ions which was calculated by the MCDF method (Indelicato et al. 1989) and later by RMBPT (Johnson et al. 1997). This effect was then observed in a variety of ions from nickel to gold (Marrus et al. 1989, Dunford et al. 1991, Indelicato et al. 1992, Birkett et al. 1993, Toleikis et al. 2004). Even the nuclear quadrupole moment can have a large effect for the lifetimes of metastable states (see, e.g. (Parente et al. 1994)). The most recent experiment (Toleikis et al. 2004), is the heir of the thirty-years old Beam-Foil technique. Yet its accuracy is the result of several factors. It uses the increase in the lifetime of the ion due to relativity at high-beam energies. The set-up comprises a magnetic spectrometer and an advanced position-sensitive beam detector to detect the photons from the metastable state in coincidence with ions of the associated charge-state. Finally it benefits from the high quality of electron-cooled ions beam from the SIS synchrotron in GSI.

3.4. Two-photon emission

Two-photon transitions can become important in heavy ions when a level cannot decay by other ways, e.g., when only strictly forbidden $J = 0 \rightarrow J = 0$ transitions would be possible otherwise. The $2E_1$ two-photon transition, for instance, dominate the lifetimes of the $2s$ and $1s2s\ ^3S_1$ levels at low- Z , but not at high- Z , because of the strong Z -dependence of the M_1 transition. In the absence of nuclear magnetic moments, the $1s2s\ ^1S_0$ level decays mostly by a two-photon transition to the $1s^2\ ^1S_0$ ground-state level. For such two-photon transitions, however, probabilities are difficult to calculate and to measure since the two-photon spectrum is spread between zero and the energy difference between the initial and final levels. Early experiments looked at the single-photon spectrum, which requires a very good signal to noise ratio, and a large effort to reduce contaminant X-rays from the envioning material. The heaviest highly charged ions studied by this method was helium-like Kr (Marrus et al. 1986). More recently a coincidence technique was applied where the two emitted photon are detected by two different detectors. Requiring that the sum of the two-photon energy is equal to the transition energy, the spectral shape of the continuum distribution of the $2E_1$ decay was

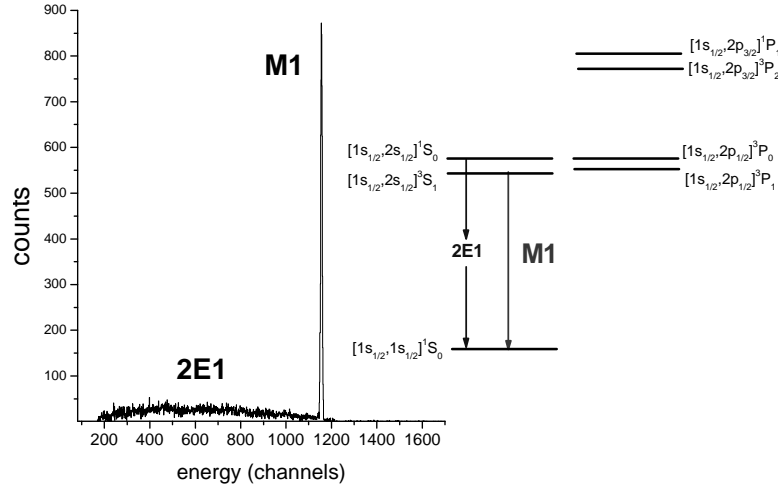


Figure 5. X-ray spectrum observed for Li-like uranium U^{89+} in collisions with N_2 , measured in coincidence with the projectile ionization, i.e. U^{90+} . The spectrum is entirely governed by a single $K\alpha$ transition stemming from the M_1 decay of the $1s2s\ ^3S_1$ state. The broad feature is due to the two-photon decay ($2E_1$) of the $1s2s\ ^1S_0$ level.

analyzed and provided accurate results for heavy elements (Schffer et al. 1999). From the theoretical point of view, the transition probability of two-photon transitions is calculated by second-order perturbation theory. Both, the positive and negative energy states must be included in order to have a good correspondence between the different gauges. The relativistic rates and photon distribution shapes for the $2s \rightarrow 1s$ transition in hydrogenlike ions have been recalculated recently, taking into account QED correction to the energy and the nine first multipole contributions (Santos et al. 1998). As in the one-photon case, the E_1M_2 correction to the dominant $2E_1$ ranges from a relative contribution of 3×10^{-11} at $Z = 1$ to 0.2 % at $Z=92$. The two-photon decay rates of several helium-like levels $1s2s\ ^1S_0$, $1s2s\ ^3S_1$ (Derevianko & Johnson 1997) and $1s2p\ ^3P_0$ (Savukov & Johnson 2002) have been evaluated in a relativistic framework. In the latter work, it was found that the negative energy continuum contributes significantly to the the E_1M_1 rate from the $1s2p\ ^3P_0$ to the ground state. It should be noted that this two-photon contribution, in competition with the E_1 transition $1s2p\ ^3P_0 \rightarrow 1s2s\ ^3S_1$, represents 47 % of the $1s2p\ ^3P_0$ lifetime at $Z = 92$. Detailed measurements of the shape of the two-photon spectrum for different multiplicities and their comparison with the recent calculations quoted above remain to be done.

An example for a two-photon spectrum is shown in figure 5 in which two decay modes, the $2E_1$ transition from the $1s2s\ ^1S_0$ state and the M_1 decay of the $1s2s\ ^3S_1$ level are seen simultaneously. In this figure, the x-ray spectrum observed for Li-like uranium U^{89+} in collisions with N_2 is displayed which was measured in coincidence with projectile ionization (U^{90+}). The spectrum is entirely governed by an intense single $L \rightarrow K$ transition and a broad continuum distribution. Because we are dealing with He-like uranium produced by K-shell ionization of the Li-like species and initially in the $1s^2s$ ground state, the broad continuum can only be explained by the two-photon ($2E_1$)

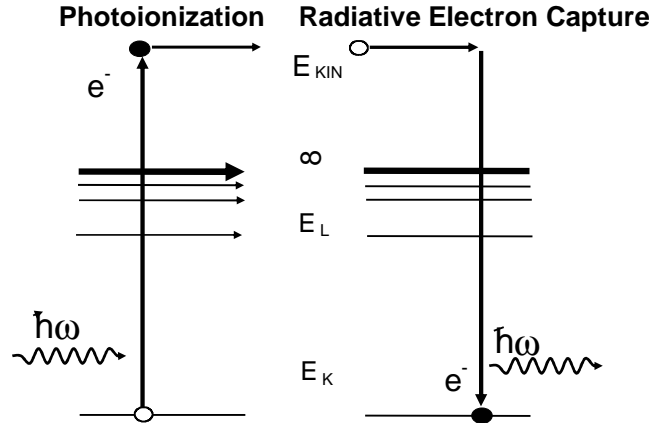


Figure 6. Radiative Electron Capture can be viewed as the time-reversed photoionization which results in an electron capture into a bound state of the ion via simultaneous emission of a photon.

decay of the $1s2s\ ^1S_0$ level while the single $K\alpha$ line arises exclusively from the M_1 decay of the $1s2s\ ^3S_1$ state. To the best of our knowledge, no other ion-atom collisions is known which produces inner-shell excited states with such a high state selectivity. This unexpected result is currently the subject of detailed theoretical investigations.

4. Electron capture into highly-charged ions

Apart from the bound-state energies and transitions, strong relativistic effects become visible also in collisions of high- Z , few-electron ions with electrons and low- Z target atoms. In these collisions, the electromagnetic field of the fast-moving projectiles often causes an ionization or capture of electrons. In particular, the radiative electron capture (REC) into bare and hydrogen-like high- Z ions has been found to provide a unique tool for studying the electron-photon interaction in the presence of strong fields.

4.1. Radiative electron capture

REC into highly-charged ions has been investigated since a long time as it represents the dominant charge exchange process for bare and H-like ions in collisions with low- Z targets at high energies (Schnopper et al. 1972, Spindler et al. 1979, Anholt et al. 1984, Stöhlker et al. 1992, Stöhlker et al. 1995, Vane et al. 2000). In this radiative recombination (RR) process, a free or quasi-free electron is captured into a bound state of the ion under the simultaneous emission of a photon. In fact, the radiative recombination of (heavy) ions with free electrons is known also as the time-reversed photo-effect. Besides the total REC cross sections, which determine the lifetimes of the ion beams at accelerators and storage rings, a number of angular distribution (Anholt et al. 1984, Stöhlker et al. 2001) and, more recently, polarization measurements have been carried out (Stöhlker et al. 2004, Tachenov et al. 2004) and have shown,

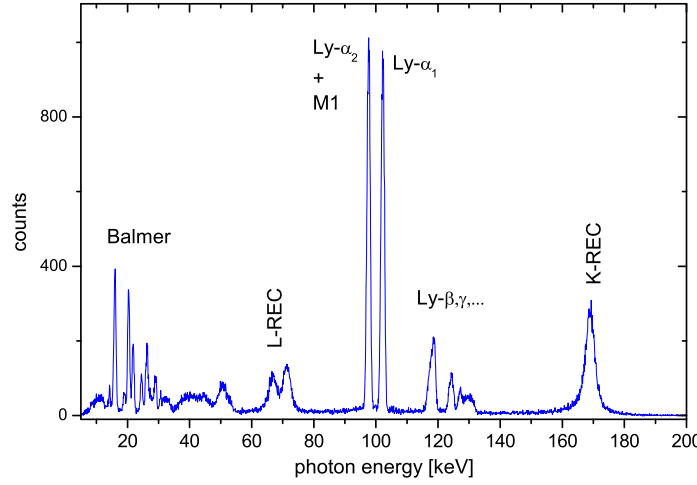


Figure 7. An x-ray spectrum associated with capture for 68 MeV/u U^{92+} on N_2 is shown. The data were taken at the ESR storage ring at an observation angle of $\theta=132^\circ$ (not corrected for detection efficiency). The x-ray energies in the laboratory frame are given (Stöhlker et al. 1998).

that the radiative capture of electrons is a powerful tool for precise studies on atomic photoionization with high-energy photons in the strong-field domain. Since the very first observations of REC (RR) photons (Schnopper et al. 1972), therefore, this process has been studied intensively for various bare and few-electron ions, including bare uranium and projectile energies from a few MeV/u up to the extrem relativistic regime above 100 GeV/u (Vane et al. 2000).

As an example, Figure 7 displays the x-ray spectrum of H-like uranium which was produced by electron capture in U^{92+} collision with N_2 at 68 MeV/u (recorded at an observation angle of 132°). As in the case of photoionization, the energy of the REC photons, $\hbar\omega_{\text{REC}} = E_b + E_{\text{kin}}$, is given by the sum of the binding energy E_b and the kinetic energy E_{kin} of the free electron in the projectile frame (in the present experiment the kinetic electron energy E_{kin} amounts to ≈ 37 keV). For the REC transitions into the $1s$ ground state of hydrogen-like uranium ($E_{1s} \approx 132$ keV), the K-REC peak is thus found in the high-energy part of the spectrum, at a photon energy of around 170 keV. Hereby, the broadening of these K-REC lines (compared to the characteristic transitions) is due to the momentum distribution of the target electrons (Compton profile).

Because of the relatively low velocity of the decelerated ions, the two $j = 1/2$ and $j = 3/2$ fine-structure components of the L-REC x-ray lines around 50 keV are still resolved and are separated by ~ 4.5 keV. This illustrates one of the benefits of using deceleration techniques in REC experiments, while the large line broadening at high projectile energies, caused by the Compton profile, often prevents the separation of the fine structure components (Stöhlker et al. 1998). The L-shell fine structure splitting, in addition, also leads to an energy separation of the two Lyman- α ground-state transitions

(Ly- $\alpha_2 + M_1$: $2p_{1/2}, 2s_{1/2} \rightarrow 1s_{1/2}$, and Ly- α_1 : $2p_{3/2} \rightarrow 1s_{1/2}$) which constitute the most intense x-ray lines in the spectrum.

On the left side of Fig. 8, the K-REC angular distribution for the capture into 88 MeV/u U^{92+} ions is shown as function of the photon emission angle in the laboratory frame (solid circles) and are compared with rigorous relativistic calculations (Stöhlker et al. 2001). As for the structure calculations in Sec. 3, a relativistic treatment of the electrons and the electron-photon interaction is typically required in order to understand the observed data from the collision experiments (Ichihara et al. 1994, Eichler & Meyerhof 1995, Ichihara et al. 1996). As seen from the figure, moreover, the measured angular distribution confirms well the slight asymmetry with respect to a perpendicular photon emission as predicted by theory. Most remarkable, however, is the non-vanishing cross section close to 0° , which demonstrates that the magnetic contributions are still present in the low-energy domain. Since the magnetic multipoles contribute 3 % to the total K-REC cross-section (cf. the dashed area in Fig. 8), this enhancement of the photon emission in forward direction shows the sensitivity of the applied method. Note that the (almost) symmetrical angular distribution with respect to 90° is a particular feature of the laboratory frame which arises from the cancellation of the various effects due to the retardation of the electron-photon interaction and the Lorentz transformation for going from the projectile to the laboratory framework, a behaviour which was predicted already by the non-relativistic theory (Spindler et al. 1979, Anholt et al. 1984).

In the emitter frame, in contrast, a strong variation occurs for the angular distribution of the emitted photons as function of the projectile energies. This is illustrated in Fig. 8(right side) where the observed data are Lorentz-transformed into the projectile frame. Even for the low energy regime where the kinetic electron energy E_{kin} is much smaller than the binding energy in the final state E_b , that is for a photoionization close to the threshold (Stöhlker et al. 2001), the angular distribution still exhibits a considerable backward peaking in accordance with the enhanced forward emission in the direct photoionization process. This behaviour of the angular distribution can be understood easily by replacing θ' by $\pi - \theta'$ as indicated on the upper abscissa of Figure 8. Theoretically, the radiative electron capture and all the subsequent emission processes are most easily described by means of the density matrix theory where, instead of a single collision event, an ensemble of (equally prepared) systems is considered. As appropriate for collision processes, these systems can be either in a *pure* quantum state or in a *mixture* of different states with any degree of coherence (Blum 1982, Balashov et al. 2000). Density matrix theory helps to accompany such collision ensembles through one or several regions of the interaction without losing important information about the reaction products. To support detailed collision studies, the concepts of the density matrix has been implemented meanwhile into a number of codes which are suitable for both, one- and few-electron ions (Fritzsche 2001, Surzhykov et al. 2004b).

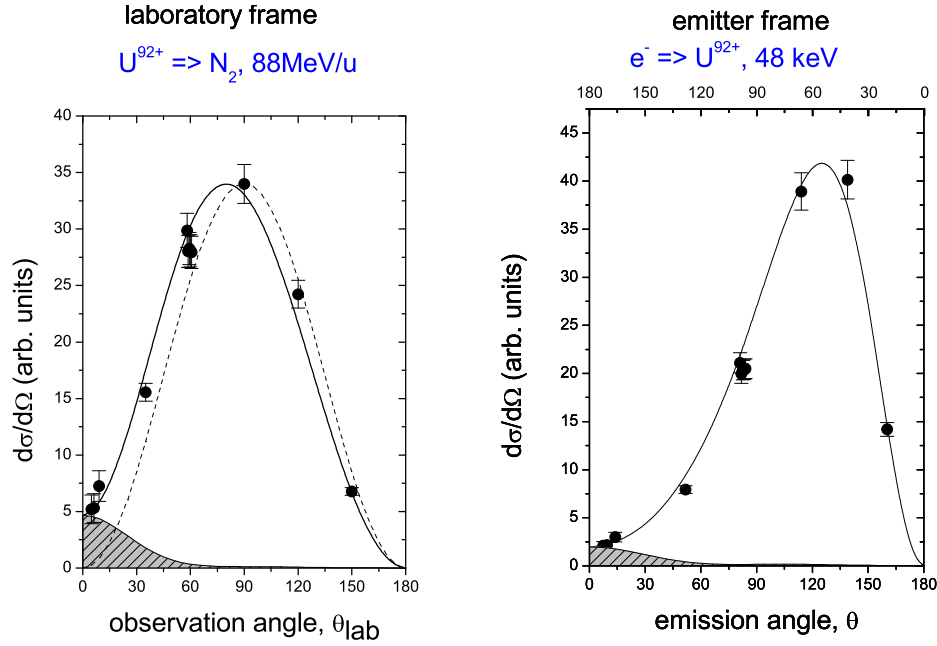


Figure 8. left side: Angular distributions for K-REC at 88 MeV/u $U^{92+} \rightarrow N_2$ collisions (Stöhlker et al. 2001). Solid circles: experimental result; solid line: relativistic calculations; shaded area: spin-flip contributions. Right side: K-REC distribution (solid circles) in the emitter frame as a function of the emission angle θ (bottom axis). The horizontal axis at the top refers to the corresponding electron emission angle in photoionization of U^{91+} (photoelectron energy: 48 keV).

4.2. Polarization studies for the K-shell capture

Details about the radiative capture can be derived not only from the angular distribution of the emitted photons but also from their polarization (Surzhykov et al. 2001, Eichler & Ichihara 2002). In practice, however, polarization measurements have been hampered in the past years because of the lack of efficient Compton polarimeters for photon energies of several ten or even hundred keV. For high- Z ions with photon energies above 100 keV, it was demonstrated only recently that the (linear) polarization of the emitted photons can be measured by means of a new generation of segmented germanium detectors, which allow for energy as well as position resolution (Inderhess et al. 1996, Stöhlker et al. 2003). A first series of polarization measurements were performed at GSI using these detectors (Stöhlker et al. 2003, Tachenov et al. 2004) and by applying the dependence of the angle-differential Compton scattering on the linear polarization of the incoming photons. As predicted theoretically (Surzhykov et al. 2001, Eichler & Ichihara 2002), a strong linear polarization of the K-REC photons is expected, which decreases in the forward direction as the energy of the projectiles is enlarged. For bare uranium ions at 400 MeV/u, for example, the photon polarization of the K-REC radiation has been analyzed at the jet-

target of the storage ring ESR. For this purpose, a planar germanium pixel detector was used, mounted at an observation angle of 90° . In the experiment, the photon polarization is obtained by recording events which occur simultaneously in two pixels of the detector. While one pixel is used to measure the Compton recoil electron (ΔE), the other one records the scattered photon ($\hbar\omega'$). A scatter plot of such coincident photon events is displayed in Fig. 9. The large number of events in the diagonal corresponds to events with a (constant) energy sum equal to the K-REC transition, i.e. $E_{K-REC} = \Delta E + \hbar\omega'$. It is important to mention that, for our initial energies ($E_{K-REC} \approx 250$ keV), the condition $\Delta E < \hbar\omega'$ is always fulfilled which allows us also to identify the segment where scattering takes place. The latter also explains the two maxima present in the 2D scatter plot. In Fig. 9b, we compare the coincident sum energy spectrum for scattering parallel (I_{\parallel}) and perpendicular (I_{\perp}) to the reaction plane (defined by the ion beam and the propagation direction of the K-REC photon). As seen from this figure, the K-REC radiation appears strongly polarized within the scattering plane.

Experimentally, the polarization properties of the emitted photons are usually obtained from the Stokes parameter, i.e., the intensity ratios of the light measured under different angles with respect to the reaction plane. For example, the Stokes parameter $P_1 = (I_{0^\circ} - I_{90^\circ}) / (I_{0^\circ} + I_{90^\circ})$, is obtained from the intensities *parallel* and *perpendicular* to the scattering plane, while the parameter P_2 follows from a similar intensity ratio, taken at $\chi = 45^\circ$ and $\chi = 135^\circ$, respectively. The two parameters P_1 and P_2 together describe the (degree and direction of the) *linear* polarization in the plane perpendicular to the photon momentum whereas the third parameter P_3 denotes the degree of *circular* polarization.

In the theoretical treatment of electron capture, the Stokes parameters are closely related to the photon density matrix if no further information need to be retained for the remaining ions apart from its level designation. For the capture of *unpolarized* electrons by bare ions, it was shown recently (Surzhykov et al. 2003b, Fritzsche et al. 2003), that only the Stokes parameter P_1 is non-zero (and positive for moderate projectile energies), while P_2 is identically zero. This implies that, for unpolarized electrons and ions, the polarization of the recombination photons will always be found within the reaction plane. For the capture of *polarized* electrons, in contrast, the Stokes parameter P_2 becomes non-zero, in particular at small forward angles θ_{RR} , leaving P_1 unaffected in this case. For the photon polarization, however, any non-zero P_2 parameter results in a rotation of the polarization ellipse out of the reaction plane. Owing to the symmetry of the collision system, a similar result is found if the (unpolarized) electrons are captured by a polarized ion beam. Therefore, the rotation of the polarization ellipse may serve as a unique tool for measuring the polarization properties of ion beams (Surzhykov et al. 2004a), a result which has attracted a lot of recent interest.

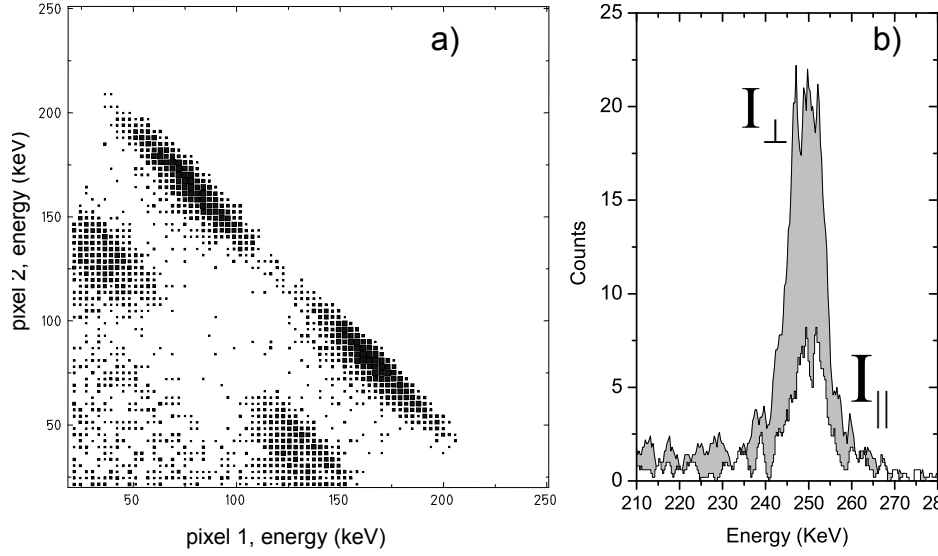


Figure 9. a) Scatter plot of coincident Compton events; b) the coincident sum energy spectrum for scattering parallel (I_{\parallel} , white area) and perpendicular (I_{\perp} , shaded area) to the scattering plane (Stöhlker et al. 2003, Tachenov et al. 2004).

4.3. Emission of characteristic radiation

If the electron is captured not into the ground state of the ion, but into an excited one, this ion state decays further towards the ground state under the emission of *characteristic* radiation. For high- Z ions, in particular, the capture into the $2p_{3/2}$ level and its subsequent Lyman- α_1 decay into the $1s$ ground state has been explored in great detail. The angular distribution of this characteristic radiation,

$$W_{\text{Ly}}(\theta) = W_o (1 + \beta_{\text{exp}} P_2(\cos \theta)) , \quad (1)$$

then allows to derive an (experimental) anisotropy parameter β_{exp} as function of the charge and the energy of the projectiles [cf. Fig. 8]. When compared to the standard dipole approximation $\beta = \mathcal{A}_2/2$, however, deviations of up to 30 % were found for the anisotropy parameters β_{exp} , where \mathcal{A}_2 refers to the alignment of the $2p_{3/2}$ level following the radiative electron capture (Stöhlker et al. 1997, Eichler et al. 1998). Initially, this large discrepancy was quite surprising since, even for hydrogen-like uranium, the dipole approximation to the electron-photon interaction was known to provide (theoretical) lifetimes with an accuracy of better or ~ 1 %. A detailed analysis in the framework of the density matrix theory later showed, however, that the increase in the observed anisotropy arises entirely from the weak M_2 branch of the Lyman- α transitions, i.e. from the interferences of the E_1 and M_2 multipole components (Surzhykov et al. 2002a). Theoretically, this enhancement is understood if, instead of the alignment \mathcal{A}_2 and anisotropy parameters β , the two *effective* parameters

$$\mathcal{A}_2^{(\text{eff})} = \mathcal{A}_2 \cdot f(E_1, M_2); \quad \beta_{20}^{(\text{eff})} = \beta_{20} \cdot f(E_1, M_2)$$

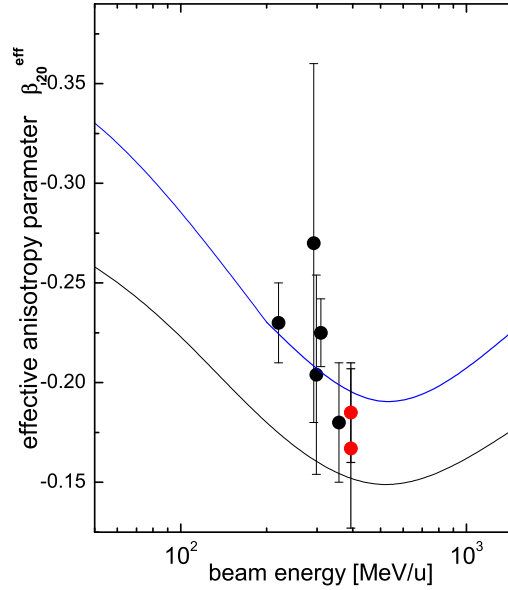


Figure 10. Comparison of experimental and theoretical (effective) anisotropy parameters β as function of the projectile energy for the Lyman- α_1 radiation of U^{91+} ions, produced in $U^{92+} \rightarrow N_2$ collisions. The lower line represents the theoretical prediction from the electric dipole approximation, while the upper line also includes the E_1 - M_2 interference (Stöhlker et al. 1997, Surzhykov et al. 2002a).

are used in Eq. (1), where

$$f(E_1, M_2) \propto \left[1 + 2\sqrt{3} \frac{\langle ||M_2|| \rangle}{\langle ||E_1|| \rangle} \right]$$

is called the structure function. This structure function purely depends on the bound-state structure of the ion, while the alignment parameters \mathcal{A}_{20} and β are of dynamical origin and, hence, are determined by the capture process. The structure function $f(E_1, M_2)$ is roughly proportional to Z^2 and, therefore, non-negligible effects of a few percent from the M_2 multipole component may arise even for medium- Z ions.

Apart from the incorporation of higher multipoles, there is an alternative view of how such *interference* effects in high- Z ions can be used to obtain insight into the interaction with the radiation field. If we assume, for instance, that the REC into bare ions is well understood by means of the (relativistic) density matrix theory, we may utilize the theoretical alignment for the capture into the $2p_{3/2}$ level in order to derive the structure function $f(E_1, M_2)$ also experimentally. Applied to the angular distribution data from Fig. 10, a value $f^{(\text{exp})}(E_1, M_2) = 1.27 \pm 0.05$ is obtained, giving rise to a relative contribution of the M_2 decay branch of $\Gamma_{M_2}/\Gamma_{E_1} = 0.0077 \pm 0.0009$ (Orsic-Muthig 2004).

4.4. Multiple photon emission: angular correlations

A great deal of information about the electron-photon interaction in the presence of strong fields has been obtained from the x-ray spectra of either the REC or the characteristic radiation. Further details can be derived if the photon emission from the electron capture and the subsequent bound-bound decay are observed in coincidence. Perhaps, the most simple coincidence measurement refers to the observation of the angular-angular correlations which reflect the differential alignment in the population of the magnetic sublevels as function of the observation angle of the recombination photon. For the electron capture by U^{92+} ions, a very strong dependence has been predicted for the angular distribution of the subsequent photon decay (Surzhykov et al. 2002b, Surzhykov et al. 2003a), using proper tools for the spin-angular and radial integration (Fritzsche 1997, Surzhykov et al. 2004b). Other correlation functions can be defined and may lead to additional information about the polarization properties of the emitted radiation in the future. The great advantage of such correlation studies is that they provide an alternative route for determining the polarization properties of the (heavy) ions beams at storage rings.

5. Conclusions and outlook

The photon emission from highly-charged heavy ions has been reviewed as observed at storage rings. Studies on both, the bound-bound and free-bound transition in high- Z ions, have revealed many details and have improved the understanding of the electron-photon interaction in the strong-fields domain. These investigations clearly show the inherently *relativistic* behavior of all the structure and collision processes observed in high-energy atomic physics. In studying high- Z ions, the role of Quantum Electrodynamics becomes predominant. It is thus confirmed as the fundamental theory for describing atomic and ionic systems.

For the capture of electrons into ionic bound states, an interference has been seen between the different multipole components in the expansion of the radiation field. These interference effects have extended our knowledge about the photoionization of atoms and ions to much higher energies than available for the neutral elements. They demonstrate that magnetic and higher-order contributions of the radiation field may survive even for energies close to the threshold. Although these interference effects are observed so far only for the Lyman- α decay of hydrogen-like uranium, following the electron capture into the $2p_{3/2}$ level, they are important also for other few-electron systems if — apart from the leading E_1 multipole — other multipole(s) are allowed additionally. For the emitted photons, then, both the angular distributions and the polarization properties are likely to be affected.

There are further challenges to be faced in the forthcoming years, when studying fundamental processes of high- Z ions. For the radiative recombination, coincidence and polarization measurements will further advance our knowledge about the electron-

photon interaction as they are sensitive to different components of the radiation field. As outlined above, moreover, REC may provide a tool for the diagnostics and detection of spin-polarized ions in atomic collisions. When compared with accurate theoretical predictions, the observation of the photon polarization then may help to control the ion polarization in heavy-storage rings, a topic which has recently attracted much attention in atomic and nuclear physics. With control on both, the generation and the measurement of polarized ion beams, a whole class of new experiments will become feasible, including the study of parity non-conserving (PNC) effects (Maul et al. 1996) or the search for electric dipole moments of highly-charged ions. Experimentally, ideal conditions for such challenging studies will be provided by the new heavy ion facilities presently under discussion, such as the new international accelerator Facility for Antiproton and Ion Research (FAIR) at GSI (Henning 2001). There highest intensities for beams of both stable and exotic heavy nuclei will become available.

Acknowledgments

This work has been supported by the BMBF, the GSI and the Laboratoire Kastler Brossel (Unité Mixte de Recherche du CNRS n° 8552).

References

- Anholt R, Andriamonje S A, Morenzoni E, Stoller C, Molitoris J D, Meyerhof W E, Dowman H, Xu J S, Xu Z Z, Rasmussen J O & Hoffmann D H H 1984 *Phys. Rev. Lett.* **53**, 234.
- Åsén B, Salomonson S & Lindgren I 2002 *Phys. Rev. A* **65**(3), 032516 (16).
- Balashov V V, Grum-Grzhimailo A N & Kabachnik N M 2000 *Polarization and Correlation Phenomena in Atomic Collisions. A Practical Theory Course* Kluwer Academic New York.
- Beiersdorfer P, Knapp D, Marrs R E, Elliot S R & Chen M H 1993 *Phys. Rev. Lett.* **71**(24), 3939–3942.
- Beiersdorfer P, Osterheld A, Elliott S R, Chen M H, Knapp D & Reed K 1995 *Phys. Rev. A* **52**(4), 2693–2706.
- Beiersdorfer P, Osterheld A L, Scofield J, Wargelin B & Mars R E 1991 *Phys. Rev. Lett.* **67**(17), 2272–2275.
- Bethe H A 1947 *Phys. Rev.* **72**(4), 339341.
- Beyer H, Stöhlker T, Banas D, Liesen D, Protic D, Beckert K, Beller P, Bojowald J, Bosch F, Förster E, Franzke B, Gumberidze A, Hagmann S, Hoszowska J, Indelicato P, Klepper O, Kluge H J, König S, Kozhuharov C, Ma X, Manil B, Mohosc I, Orsic-Muthig A, Nolden F, Popp U, Simionovici A, Sierpowski D, Spillmann U, Stachura Z, Steck M, Tachenov S, Trassinelli M, Warczak A, Wehrhan O & Ziegler E 2004 *Spectrochimica Acta Part B* p. 1535.
- Birkett B B, Briand J P, Charles P, Dietrich D D, Finlayson K, Indelicato P, Liesen D, Marrus R & Simionovici A 1993 *Phys. Rev. A* **47**(4), R2454–R2457.
- Blum K 1982 *Density Matrix Theory and Applications* Plenum Press New York.
- Blundell S A, Mohr P, Johnson W R & Sapirstein J 1993 *Phys. Rev. A* **48**(4), 2615–2626.
- Bosch F 1993 *AIP Conference Proceedings* **295**, 3.
- Brandau C, Kozhuharov C, Müller A, Shi W, Schippers S, Bartsch T, Böhm S, Böhme C, Hoffknecht A, Knopp H, Grün N, Scheid W, Steih T, Bosch F, Franzke B, Mokler P H, Nolden F, Steck M, Stöhlker T & Stachura Z 2003 *Phys. Rev. Lett.* **91**(7), 073202.
- Breit G 1929 *Phys. Rev.* **34**, 375.
- Briand J P, Chevallier P, Indelicato P, Dietrich D & Ziock K 1990 *Phys. Rev. Lett.* **65**(22), 2761–2764.

- Brown G E & Ravenhall D E 1951 *Proc. R. Soc. London, Ser A* **208**, 552–559.
- Chen M H, Cheng K T & Johnson W R 1993 *Phys. Rev. A* **47**(5), 3692–3703.
- Chen M H, Cheng K T & Johnson W R 2001 *Phys. Rev. A* **64**(4), 042507 (7).
- Cheng K T, Chen M H, Johnson W R & Sapirstein J 1994 *Phys. Rev. A* **50**(1), 247–255.
- Cheng K T & Johnson W R 1977 *Phys. Rev. A* **16**(1), 263–272.
- Cheng K T, Johnson W R & Sapirstein J 1991 *Phys. Rev. Lett.* **66**, 2960–2963.
- Cheng K T, Johnson W R & Sapirstein J 1993 *Phys. Rev. A* **47**(3), 1817–1823.
- Derevianko A & Johnson W R 1997 *Phys. Rev. A* **56**(2), 1288–1294.
- Derevianko A, Savukov I M, Johnson W R & Plante D R 1998 *Phys. Rev. A* **58**, 4453–4461.
- Desclaux J P 1975 *Comp. Phys. Commun.* **9**, 31–45.
- Dirac P A M 1928 *Proc. Roy. Soc. London* **A117**, 610–624.
- Dunford R W, Liu C, Last J, Berrah-Mansour N, Vondrasek R, Church D A & Curtis L 1991 *Phys. Rev. A* **44**(1), 764–767.
- Eichler J & Ichihara A 2002 *Phys. Rev. A* **65**, 052716.
- Eichler J, Ichihara A & Shirai T 1998 *Phys. Rev. A* **58**, 2128.
- Eichler J & Meyerhof W 1995 *Relativistic Atomic Collisions* Academic Press San Diego.
- Franzke B 1987 *Nucl. Instr. Meth. B* **24/25**, 18.
- Franzke B 1990 *Physics Reports* **196**, 135.
- Fritzsche S 1997 *Comp. Phys. Commun.* **103**, 51.
- Fritzsche S 2001 *J. Electr. Spectr. Rel. Phenom.* **114-116**, 1155.
- Fritzsche S, Surzhykov A & Stöhlker T 2003 in G. F Hanne, L Malegat & H Schmidt-Böcking, eds, ‘Correlation and Polarization in Photonic, Electronic, and Atomic Collisions’ Vol. 697 AIP Conference Proceedings New York p. 102.
- Gillaspay J 2001 *Trapping Highly Charged Ions: Fundamentals and Applications* Nova Science Publishers.
- Grant I P 1970 *Adv. Phys.* **19**, 747.
- Gumberidze A, Stöhlker T, Banaś D, Beckert K, Beller P, Beyer H F, Bosch F, Hagmann S, Kozhuharov C, Liesen D, Nolden F, Ma X, Mokler P H, Oric-Muthig A, Steck M, Sierpowski D, Tashenov S & Zou Y 2004 *Phys. Rev. Lett.* **in press**.
- Henning W 2001 *Internal Accelerator Facility for Beams of Ions and Antiprotons* GSI.
*<http://www.gsi.de/GSI-Future/cdr/>
- Heully J L, Lindgren I, Lindroth E, Lundqvist S & Mårtensson-Pendrill A M 1986 *J. Phys. B: At. Mol. Phys.* **19**, 2799–2815.
- Heully J L, Lindgren I, Lindroth E & Mårtensson-Pendrill A M 1986b *Phys. Rev. A* **33**(6), 4426–4429.
- Ichihara A, Shirai T & Eichler J 1994 *Phys. Rev. A* **49**, 1875.
- Ichihara A, Shirai T & Eichler J 1996 *Phys. Rev. A* **54**, 4954.
- Indelicato P 1995 *Phys. Rev. A* **51**(2), 1132–1145.
- Indelicato P 1996 *Phys. Rev. Lett.* **77**(16), 3323–3326.
- Indelicato P 1997 *Hyp. Int.* **108**(1-3), 39–49.
- Indelicato P, Birkett B B, Briand J P, Charles P, Dietrich D D, Marrus R & Simionovici A 1992 *Phys. Rev. Lett.* **68**(9), 1307–1310.
- Indelicato P & Mohr P 2001 *Phys. Rev. A* **63**(4), 052507.
- Indelicato P & Mohr P J 1991 *Theor. Chem. Acta.* **80**, 207.
- Indelicato P, Parente F & Marrus R 1989 *Phys. Rev. A* **40**(7), 3505–3514.
- Indelicato P, Shabaev V M & Volotka A V 2004 *Phys. Rev. A* **69**(6), 062506–9.
- Inderhess S E, Philips B, Kroeger R A, Johnson W N, Kinzer R L, Kurfess J D, Graham B & Gehrels N 1996 *EEE Trans. on Nuclear Science* **43**, 1467.
- Johnson W R, Blundell S & Sapirstein J 1988 *Phys. Rev. A* **37**(8), 2764–77.
- Johnson W R, Cheng K T & Plante D R 1997 *Phys. Rev. A* **55**(4), 2728–2742.
- Johnson W R, Plante D R & Sapirstein J 1995a in B Bederson & H Walters, eds, ‘Advances in Atomic, Molecular and Optical Physics’ Vol. 35 Addison-Wesley New York pp. 255–329.
- Johnson W R, Sapirstein J & Cheng K T 1995 *Phys. Rev. A* **51**(1), 297–302.

- Kelly H P 1963 *Phys. Rev.* **131**(2), 684–699.
- Lamb W E & Retherford R C 1950 *Phys. Rev.* **79**(4), 549–572.
- Lindgren I 1974 *J. Phys. B: At. Mol. Opt. Phys.* **7**(18), 2441–2470.
- Lindgren I 2000 *Mol. Phys.* **98**(16), 1159–1174.
- Lindgren I, Persson H, Salomonson S & Labzowsky L 1995 *Phys. Rev. A* **51**(2), 1167–1195.
- Lindgren I, Salomonson S & Åsén B 2004 *Phys. Rep.* **389**(4), 161–261.
- Marrs R E, Beiersdorfer P & Schneider D 1994 *Physics Today* **October**, 27.
- Marrs R E, Elliott S R & Knapp D A 1994 *Phys. Rev. Lett.* **72**, 4082.
- Marrus R, Charles P, Indelicato P, de Billy L, Tazi C, Briand J P, Simionovici A, Dietrich D, Bosch F & Liesen D 1989a *Phys. Rev. A* **39**, 3725.
- Marrus R & Mohr P 1978 *Adv. At. Mol. Phys.* **14**, 181–224.
- Marrus R, San Vicente V, Charles P, Briand J P, Bosch F, Liesen D & Varga I 1986 *Phys. Rev. Lett.* **56**(16), 1683.
- Marrus R, Simionovici A, Indelicato P, Dietrich D D, Charles P, Briand J P, Finlayson K, Bosch F, Liesen D & Parente F 1989 *Phys. Rev. Lett.* **63**(5), 502–504.
- Maul M, Schäfer A, Greiner W & Indelicato P 1996 *Phys. Rev. A* **53**(6), 3915–3925.
- Mohr P J 1974 *Ann. Phys. (N.Y.)* **88**, 52.
- Mohr P J & Sapirstein J 2000 *Phys. Rev. A* **62**(5), 052501.
- Mohr P, Plunien G & Soff G 1998 *Phys. Rep.* **293**, 227–372.
- Mokler P H & Stöhlker T 1996 *Advances in Atomic and Molecular Physics* **37**, 297.
- Orsic-Muthig A 2004. Dissertation, University of Frankfurt, to be published.
- Parente F, Marques J P & Indelicato P 1994 *Europhys. Lett.* **26**(6), 437–442.
- Plunien G & Soff G 1995 *51* **2**(51), 1119–1131.
- Protic D, Stöhlker T, Beyer H F, Bojowald J, Borchert G, Hamacher A, Kozhuharov C, Ludziejewski T, Ma X & Mohos I 2001 *IEEE Transactions on Nuclear Science* **48**, 1048.
- Saathoff G, Karpuk S, Eisenbarth U, Huber G, Krohn S, Muoz Horta R, Reinhardt S, Schwalm D, Wolf A & Gwinner G 2003 *Phys. Rev. Lett.* **91**(19), 190403.
- Santos J P, Parente F & Indelicato P 1998 *Eur. Phys. J. D* **3**(1), 43–52.
- Sapirstein J 1998 *Rev. Mod. Phys.* **70**(1), 55–76.
- Sapirstein J, Pachucki K & Cheng K T 2004 *Phys. Rev. A* **69**(2), 022113–10.
- Savukov I M & Johnson W R 2002 *Phys. Rev. A* **66**(6), 062507 (5).
- Schneider M D, Levine M A, ad J. R. Henderson C L B, Knapp D A & Marrs R E 1989 *AIP Conf. Proc.* p. 188.
- Schnopper H, Betz H, Devaille J, Kalata K, Sohval A R, Jones K & Wegner H E 1972 *Phys. Rev. Lett.* **29**.
- Schweppe J, Belkacem A, Blumenfeld L, Claytor N, Feynberg B, Gould H, Kostroun V, Levy L, Misawa S, Mowat R & Prior M 1991 *Phys. Rev. Lett.* **66**(11), 1434–1437.
- Schffer H, Mokler P, Dunford R, Kozhuharov C, Krämer A, Ludziejewski T, Prinz H T, Rymuza P, Sarkadi L, Stöhlker T, Swiat P & Warczak A 1999 *Physica Scripta T* **80**, 469.
- Shabaev V 1990 *Soviet Physics Journal* **33**(8), 660–670.
- Spindler E, Betz H D & Bell F 1979 *Phys. Rev. Lett.* **42**, 832.
- Steck M, Beller P, Beckert K, Franzke B & Nolden F 2004 *Nucl. Instr. Meth. A* **532**, 357.
- Stöhlker T, Banas D, Fritzsche S, Gumberidze A, Kozhuharov C, Ma X, Orsic-Muthig A, Spillmann U, Sierpowski D, Surzhykov A, Tachenov S & Warczak A 2004 *Physica Scripta T* **110**, 384.
- Stöhlker T, Banas D, Gumberidze A, Kozhuharov C, Krings T, Lewoczko W, Ma X, Protic D, Sierpowski D, Tachenov S & Warczak A 2003 *Nucl. Instr. Meth. B* **205**, 210.
- Stöhlker T, Bosch F, Gallus A, Kozhuharov C, Menzel G, Mokler P H, Prinz H T, Eichler J, Ichihara A, Shirai T, Dunford R, Ludziejewski T, Rymuza P, Stachura Z, Swiat P & Warczak A 1997 *Phys. Rev. Lett.* **79**, 3270.
- Stöhlker T, Kozhuharov C, Livingston A E, Mokler P H, Stachura Z, & Warczak A 1992 *Z. Phys. D* **23**, 121.

- Stöhlker T, Kozhuharov C, Mokler P H, Warczak A, Bosch F, Geissel H, Scheidenberger C, Moshhammer R, Eichler J, Ichihara A, Shirai T, Stachura Z & Rymuza P 1995 *Phys. Rev. A* **51**, 2098.
- Stöhlker T, Ludziejewski T, Reich H, Bosch F, Dunford R, Eichler J, Franzke B, Kozhuharov C, Menzel G, Mokler P H, Nolden F, Rymuza P, Stachura Z, Steck M, Swiat P & Warczak A 1998 *Phys. Rev. A* **58**, 2043.
- Stöhlker T, Ma X, Ludziejewski T, Beyer H F, Bosch F, Brinzaescu O, Dunford R W, Eichler J, Hagmann S, Ichihara A, Kozhuharov C, Kramer A, Liesen D, Mokler P H, Stachura Z, Swiat P & Warczak A 2001 *Phys. Rev. Lett.* **86**(6), 983–986.
- Sucher J 1980 *Phys. Rev. A* **22**(2), 348–362.
- Surzhykov A, Fritzsche S, Gumberidze A & Stöhlker T 2002a *Phys. Rev. Lett.* **88**, 153001.
- Surzhykov A, Fritzsche S & Stöhlker T 2001 *Phys. Lett.* **A289**, 213.
- Surzhykov A, Fritzsche S & Stöhlker T 2002b *J. Phys. B: At. Mol. Opt. Phys.* **35**, 3713.
- Surzhykov A, Fritzsche S & Stöhlker T 2003a *Nucl. Instr. Meth.* **B205**, 391.
- Surzhykov A, Fritzsche S, Stöhlker T & Tachenov S 2003b *Phys. Rev.* **A68**, 022719.
- Surzhykov A, Fritzsche S, Stöhlker T & Tachenov S 2004a *Phys. Rev. Lett.* p. submitted.
- Surzhykov A, Koval P & Fritzsche S 2004b *Comp. Phys. Commun.* p. in print.
- Swirles B 1935 *Proc. R. Soc. London, Ser A* **152**, 625.
- Tachenov S, Stöhlker T, Gumberidze A, Spillmann U, Banas D, Kozhuharov C, Protic D, Krings T & Sierpowski S 2004 **to be published**.
- Toleikis S, Manil B, Berdermann E, Beyer H F, Bosch F, Czanta M, Dunford R W, Gumberidze A, Indelicato P, Kozhuharov C, Liesen D, Ma X, Marrus R, Mokler P H, Schneider D, Simionovici A, Stachura Z, Stöhlker T, Warczak A & Zou Y 2004 *Phys. Rev. A* **69**(2), 022507–5.
- Uehling E A 1935 *Phys. Rev.* **48**, 55–63.
- Vane C R, Krause H F, Datz S, Grafström P, Knudsen H, Scheidenberger C & Schuch R H 2000 *Phys. Rev. A* **62**.
- Yerokhin V A, Artemyev A N, Beier T, Shabaev V M & Soff G 1998 *J. Phys. B: At. Mol. Opt. Phys.* **31**, L691–697.
- Yerokhin V A, Artemyev A N, Beier T, Shabaev V M & Soff G 1999 *Phys. Scr.* **80B**, 495–497.
- Yerokhin V A, Artemyev A N, Shabaev V M, Sysak M M, Zhrebtsov O M & Soff G 2000 *Phys. Rev. Lett.* **85**(22), 4699–4702.
- Yerokhin V A, Indelicato P & Shabaev V M 2003a *Eur. Phys. J. D* **25**(3), 203–238.
- Yerokhin V A, Indelicato P & Shabaev V M 2003b *Phys. Rev. Lett.* **91**(7), 073001.